Jpn. J. Vet. Res., **35**, 21–39 (1987)

FOX MINUTE VIRUS-LIKE PARTICLE

Hiroshi KITAGAWA,[1] Hiroshi SATOH,[2] Chiyoko KOMATSUZAKI[2]
Fumiaki MORI[2] and Norio KUDO[1]

(Accepted for publication November 27, 1986)

Morphological investagations were carried out on basophilic intranuclear and cytoplasmic inclusion bodies in epithelial cells of the hair bulbs of anagen hair follicles in wild foxes affected with an abnormal hair coat condition. The inclusions, which were DNA-positive, contained numerous minute virus-like particles ("FMVP"). The particles, having a diameter of approximately 13 nm, had an arrangement of capsomer-like subunits of approximately 2–3 nm in diameter and were nonenveloped. The striking resemblance to icosahedral virus was crystallographically and morphologically demonstrated.

Key words: fox leucotrichia, leucomyelo-degeneration, hair bulbs, DNA-positive inclusion, virus-like particle

INTRODUCTION

Wild foxes, *Vulpes vulpes schrencki* KISHIDA, 1924, which in winter have an abnormal hair coat condition consisting of leucotrichia, hypotrichosis and incomplete shedding of the primary hairs, have been noted in northern Hokkaido, Japan, in recent years. Fifty three foxes affected with the condition, including 136 that were killed in the Soya district of northern Hokkaido in 1981, have been recorded.

The present paper describes some of the morphological characteristics of "fox minute virus-like particle", which made up the intranuclear and cytoplasmic inclusion bodies seen in hair follicles from the affected foxes.

MATERIALS AND METHODS

Thirteen foxes affected with the abnormal hair coat condition, weighing 4–7kg, were shot dead in the winters of 1981–1983 and examined pathologically.

Light microscopy Examinations were performed in various regions of the skin throughout the whole body and in all of the segments from the cervical to the lumbar parts of the spinal cord in all 13 animals. Section preparations were stained with hematoxylin-eosin, luxol fast blue, Bodian stain and Feulgen reaction.

Department of Veterinary Anatomy[1] & Comparative Pathology[2], Faculty of Veterinary Medicine Hokkaido University, Sapporo 060, Japan

Electron microscopy Tissue specimens from various regions of the skin thoughout the whole body of 5 randomly selected animals were fixed in 3%-glutaraldehyde in 0.1M-phosphate buffer and 1%-OsO_4 in 0.1M-phosphate buffer. The specimens were embedded in Quetol–812 mixture. Ultra thin sections were stained with uranyl acetate and lead citrate.

RESULTS

Light microscopy Almost all of the hair follicles of the 13 animals were in the telogen stage, although there were a few anagen follicles. Epithelial cells of the hair bulbs, especially the matrices of the anagen follicles, often showed hydropic degeneration or pyknosis and decrease or lack of melanin granules. These regressively changed epithelial cells often had basophilic inclusion bodies that were intranuclear in 7 animals and cytoplasmic in all 13 animals (Fig. 1). The intranuclear inclusions were either homogeneous or granular. The cytoplasmic inclusions were homogenous, with occasional fine vesicles, and they varied in shape, size and number. Both types of inclusions revealed DNA-positive staining by Feulgen reaction (Fig. 2).

The cutaneous and subcutaneous nerves sometimes showed swelling and / or vesiculation of axons. The arrector pilli muscles showed hydropic degeneration.

Detailed examinations of the spinal cord revealed slight leukomyelo-degeneration that was more severe in the dorsal funiculi (dorsal leukomyelo-degeneration) in all 13 animals. The dorso-funicular degeneration was characterized by bilateral-symmetric involvement mainly in the marginal parts of the cord, by beaded swelling and feeble staining (Bodian-unstainable) of axons and by apparently normal appearance of myelin sheaths in luxol fast blue stained preparations (Fig. 3).

Electron microscopy Epithelial cells of the hair roots, particularly the hair matrices in the anagen stage, showed hydropic degeneration. There were almost no cytoplasmic unit membranes, except for a few mitochondria and desmosomes, in the epithelial cells. The intranuclear and cytoplasmic inclusion bodies were composed primarily of aggregations of minute particles having a diameter of approximately 13 nm.

The inclusion-laden nuclei exhibited marginal hyperchromasia to loss of karyoplasm (Figs. 4a, 5a & b). The intranuclear inclusions contained orderless aggregations of the particles and irregular-shaped electron dense amorphous substances resembling fleecy clouds (Fig. 4b). The inclusion was connected to the cytoplasm probably at the nucleo-pore, where virus-like particles were found (Fig. 4c). The inclusion sometimes contained slender filaments, approximately 2 nm in diameter, which exhibited irregular distribution and direction patterns with occasional cluster formations (Fig. 5c).

The cytoplasmic inclusions contained various structures: globular structures in which the particles aggregated densely and took partially crystalline arrays (Fig. 6a & b); polygonal crystalline structures in which the particles were arranged regularly

(Fig. 7a & b); ringed structures in which the particles were arranged in a single line along a certain cytoplasmic membrane (Fig. 8a & c); ovoid structures and other structures resembling a fleecy cloud consisting of electron dense amorphous substances, along whose border the particles were arranged in single or multiple lines (Figs. 6c, 7a & b, 8b & 9). These electron dense amorphous substances always had a positional relation to the particles. The cytoplasmic inclusions were not surrounded by any unit membranes.

The minute particles sometimes showed a definitely hexagonal outline and possessed no tail (Fig. 10a). Observations by using dodecahedral and icosahedral models revealed that the particles displayed an icosahedral pattern, as viewed the icosahedral model along the three fold symmetry axis (Fig. 10b, c, d & e). The particles were often arranged in a hexagonal or square crystalline array (Fig. 11a & b). The center-to-center distance between two adjacent particles was about the same in the hexagonal and square lattices (Fig. 11c & d). High resolution electron micrographs revealed that the minute particles consisted of morphological units of approximately 2–3 nm in diameter. Employing some technical artifacts, observations were carried out to compare the arrangement of the units with an icosahedral model, which was constructed so that each vertex was occupied by one black plastic ball (Fig. 12). The arrangement of the units coincided with that of the balls when the icosahedral model was viewed along a two fold axis of symmetry, a five fold axis and an inclination of about 10.8 degrees against a five fold axis.

Minute particles without a unit membrane were also observed in the interepithelial spaces of the external root sheaths (Fig. 13a) and connective tissues around the hair bulbs (Fig. 13b).

No particles were detected in the non-affected hair follicles.

Discussion

Symmetry of the minute particle The space lattices that possess hexagonal and square lattices in several planes of three-dimensional lattices are the primitive cubic lattice and the face-centered cubic lattice. Boulanger et al. (1973 / 74) pointed out that if the distance between the centers of two neighbouring virions was found to be equal in both the hexagonal and square lattice, the crystals were possible only in the face-centered cubic system. In our computation, however, the distance in the square lattice of the face-centered cubic lattice was $\sqrt{2}$ times longer than that in the hexagonal lattice, though the distance in the square lattice was exactly equal to that in the hexagonal lattice of the primitive cubic lattice. The distance between the centers of two neighbouring particles was about the same in both the hexagonal and square lattices examined herein. This indicates that the crystalline structures within the present inclusion bodies belong to the cubic tetartohedral class, with a space group P23, No. 195.[15] Setting the origin to special positions cordinated as 0, 0, 0 (cube

corner), the present hexagonal array indicates the ($\frac{1}{2}$, $\frac{1}{2}$, $\frac{1}{2}$) planes and the square array indicates the ($\frac{1}{2}$, 0, 0) planes of the cubic system. Each plane is interpreted as being viewed along the axes of three fold symmetry and two fold symmetry respectively.[12,13,14]

HODGKIN (1950) and LOW (1953) mentioned that if the symmetry of the crystalline lattice is genuinely cubic, the virus particle might have cubic symmetry. The present minute particles composing the crystalline lattice possessed 2 and 3 fold rotational symmetry axes. Incidentally, regular polyhedra, which possess 2 and 3 fold symmetry axes and demonstrate the cubic symmetry possible for spherical virus, are correspond to tetrahedron, cube, octahedron, dodecahedron or icosahedron.

CASPER (1956) and KLUG & CASPER (1960) mentioned that virus symmetry is still higher (octahedral or icosahedral) than it determined by the crystal lattice, but it cannot be lower. The additional rotational axes characterizing icosahedral symmetry are non-crystallographic, since no space group or crystal lattice can possess 5 fold symmetry axes. CASPER (1956) pointed out that the presence of non-crystallographic axes could be detected by considering the distribution of intensity in the diffraction pattern of a crystal. In the present study, the X-ray diffraction technique was not used, but by the examining the arrangements of the morphological units, it was clear that the minute particle possessed 5 fold symmetry axes in addition to 2 and 3 fold symmetry. Though regular polyhedra, such as those possessing 532 symmetry, are correspond to dodecahedron as well as icosahedron, the present hexagonal outline of the minute particles indicated that they are more likely icosahedral than dodecahedral. Thus, the minute particles could be an icosahedral virus. The prediction of CRICK & WATSON (1956) that the small virus should have cubic symmetry, and this hypothesis is likely to apply to all small viruses which have a fixed size and shape, should be mentioned here.

Morphological units of the minute particle If the minute particles are an icosahedral virus, the morphological units should correspond to 12 capsomers, pentamers, located at each of the vertexes of the icosahedral virus, like adeno associated virus.[20] However, no morphological units corresponding to the hexamers of icosahedral virus could be found.

DNA-positive inclusion body Feulgen reaction revealed that the intranuclear and cytoplasmic inclusion bodies, which were primarily composed of minute particle aggregations, contained DNA. ·These minune particles might be a DNA virus.

Minute particle forming site The locations of the particle formations are regarded as both the nucleus and the cytoplasm, because the inclusion bodies were light and electron microscopically detected in both the nucleus and the cytoplasm. The electron dense amorphous substances in the inclusion bodies were similar to viroplasm, which is regarded as a site of virus assembly. Slender filaments in viroplasm have been seen in cells infected by mengo virus,[6] poliovirus,[7] beet western yellow virus,[8]

barley yellow dwarf virus,[9,10] cowpea severe mosaic virus and cowpea mosaic virus.[3] The possible nature of the slender filaments was discussed by Gill and Chong (1975); they demonstrated that the filaments in barley yellow dwarf virus (RNA virus) infected plant cells may represent a virus moiety, either double stranded RNA or RNA-protein complex. The appoximately 2 nm in diameter of the present slender filaments appears to be consistent with the diameter (2 nm) of extracted and negatively stained double stranded DNA.[1] Thus the present filaments could be viral DNA-strands, which may participate in the formation of the minute particles.

Size of the minute particle The smallest animal viruses are parvoviridae, which is 18–26 nm in diameter and icosahedral[19] and porcine circovirus, which is 17nm in diameter, isometric and hexagonal in profile.[21],[22] The size of the present particles, about 13nm, is smaller than that of these viruses; therefore the present particles are distinct from all known animal viruses. If compared to microviridae, which exists in bacterial virus and possesses icosahedral symmetry, 12 capsomers and a diameter of 27nm,[19] the present particles are very different in size. During 3%-glutaraldehyde fixation to epoxy embedding process biological materials shrink about 7% of the diameter.[17] Even if such artifactitious contraction exists, the minute particles are too small. The present particles might be a virus so far not encountered.

FMVP The present minute particles appear to possess morphological characteristics of virus itself. The authors termed the present particle "fox minute virus-like particle (FMVP)".

ACKNOWLEDGEMENTS

We thank Mr. Y. MIFUNE for his technical suggestions and the members of the HOKKAIDO HUNTING CLUB for their kind help in obtaining materials.

REFERENCES

1) BLADEN, H. A., BYRNE, R., LEVIN, J. G. & NIRENBERG, M. W. (1965): An electron microscopic study of a DNA-ribosome complex formed in vitro. *J. Mol. Biol.*, **11**, 78–83
2) BOULANGER, P. A., TORPIER, G. & RIMSKY, A. (1973/74): Crystallographic study of intranuclear adenovirus type 5 crystals. *Intervirology*, **2**, 56–62
3) CARR, R. J. & KIM, K. S. (1983): Ultrastructure of mixed plant virus infection: Bean yellow mosaic virus with cowpea severe mosaic virus or cowpea mosaic virus in bean. *Virology*, **124**, 338–348
4) CASPER, D. L. D. (1956): Structure of bushy shunt virus. *Nature*, **177**, 475–476
5) CRICK, F. H. C. & WATSON, J. D. (1956): Structure of small viruses. *Ibid.*, **177**, 473–475
6) DALES, S. & FRANKLIN, R. M. (1962): A comparison of the changes in fine structure of L cells during single cycles of viral multiplication, following their infection with the viruses of mengo and encephalomyocarditis. *J. Cell Biol.*, **14**, 281–302

7) DALES, S., EGGERS, H. J., TAMM, I. & PLADE, G. E. (1965): Electron microscopic study of the formation of poliovirus. *Virology*, **26**, 379–389
8) ESAU, K. & HOFFERT, L. L. (1972): Development of infection with beet western yellow virus in sugarbeet. *Ibid.*, **48**, 724–738
9) GILL, C. C. & CHONG, J. (1975): Development of the infection in oat leaves inoculated with barley yellow dwarf virus. *Ibid.*, **66**, 440–453
10) GILL, C. C. & CHONG, J. (1976): Differences in cellular ultrastructural alterations between variants of barley yellow dwarf virus. *Ibid.*, **75**, 33–47
11) HODGKIN, D. C. (1950): X-ray analysis and protein structure. *Cold Spring Harbor. Symp. Quant. Biol.*, **14**, 65–77
12) HORNE, R. W., PASQUALI-RONCHETTI, I. & HOBART, J. M. (1975): A negative staining-carbon film technique for studying viruses in the electron microscope. II. Application to adenovirus type 5. *J. Ultrastruct. Res.*, **51**, 233–252
13) HORNE, R. W., HOBART, J. M. & PASQUALI-RONCHETTI, I. (1975): A negative staining-carbon film technique for studying viruses in the electron microscope. III. The formation of two-dimensional and three-dimensional crystalline arrays of cowpea chlorotic mottle virus. *Ibid.*, **53**, 319–330
14) HORNE, R. W. (1979): The formation of virus crystalline arrays for electron microscopy and image analysis. *Adv. Virus Res.*, **24**, 173–221
15) International table for X-ray crystallography, 1965 Eds. HENRY, N. F. M. & LONSDALE, K., vol. 1, Birmingham: Kynoch Press
16) KLUG, A. & CASPER, D. L. D. (1960): The structure of small viruses. *Adv. Virus Res.*, **7**, 225–325
17) KONWINSKI, M., ABRAMCZUK, J., BARANSKA, W. & SZYMKOWIAK, W. (1974): Size changes of mouse ova during preparation for morphometric studies in the electron microscope. *Histochemistry*, **42**, 315–322
18) LOW, B. W. (1953): The structure and configuration of amino acids, peptides and proteins. In: The Proteins—Chemistry, biological activity, and methods, Vol. 1 Eds. NEURATH, H. & BAYLEY, K., New York: Academic Press
19) MATTHEWS, R. E. F. (1982): Classification and nomenclature of viruses. Fourth report of the international committee on taxonomy of viruses. *Intervirology*, **17**, Nos. 1–3, Baser: Karger
20) MAYER, H. D., JAMISON, R. M., JORDAN, L. E. & MELNICK, J. L. (1965): Structure and composition of a small particle prepared from a simian adenovirus. *J. Bacteriol.*, **90**, 235–242
21) TISCHER, I., RASCH, R. & TOCHTERMANN, G. (1974): Characterization of papovavirus- and picornavirus-like particles in permanent pig kidney cell lines. *Zentralbl. Bakteriol. Microbiol. Hyg.* [A], **226**, 153–157
22) TISCHER, I., GELDERBLOM, H., VETTERMANN, W. & KOCH, M. A. (1982): A very small porcine virus with circular single-stranded DNA. *Nature*, **295**, 64–66

EXPLANATION OF PLATES

PLATE I

Fig. 1 Basophilic intranuclear (arrow) and cytoplasmic inclusion bodies (arrow head) in regressively changed epithelial cells of a hair bulb. Hematoxylin-eosin stain, x 600

Fig. 2 DNA-positive staining of intranuclear (arrow) and cytoplasmic inclusion bodies (arrow head) in epithelial cells of a hair bulb. Feulgen reaction, x 600

Fig. 3 Dorsal funicular leukomyelo-degeneration in the dorsal funiculi (dorso-funicular degeneration). Bilateral-symmetric axon degeneration consisting of swelling and Bodian-unstainability at marginal parts of the dorsal funiculi. x 60

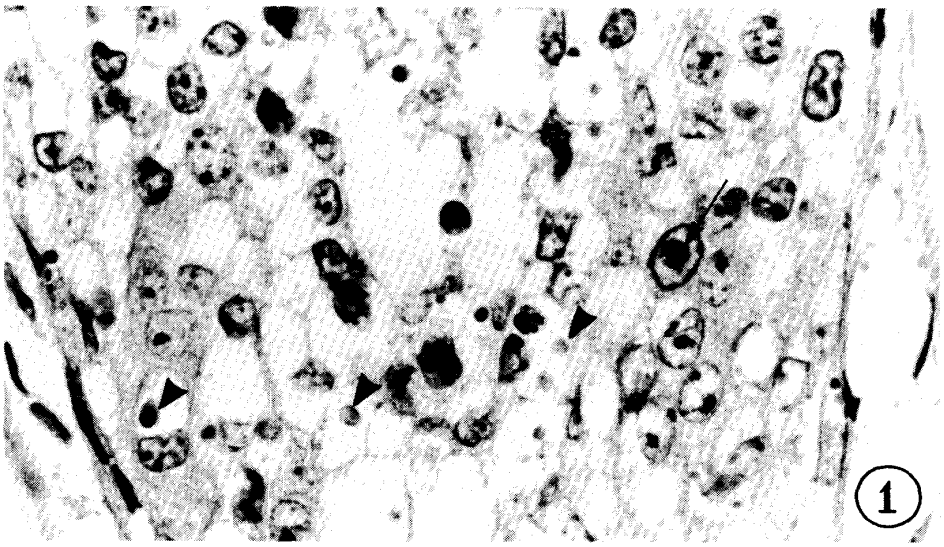

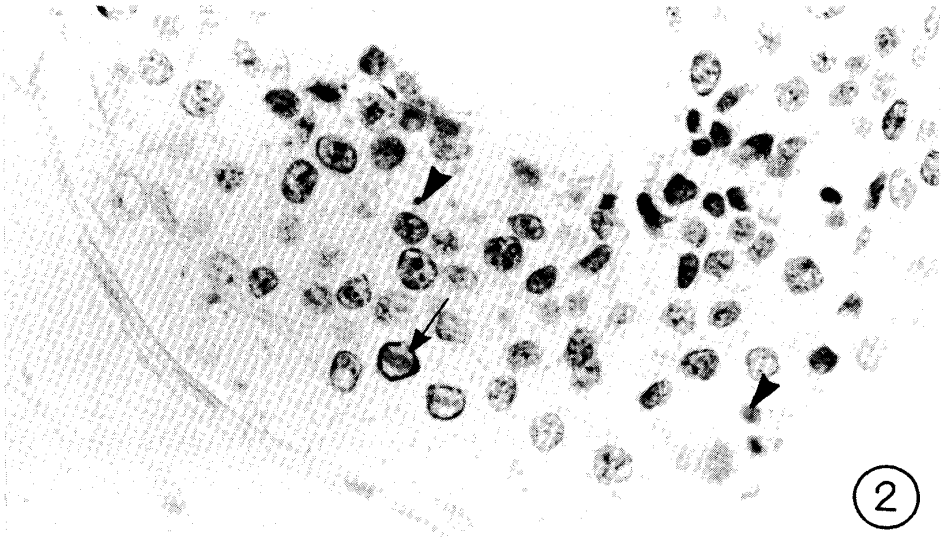

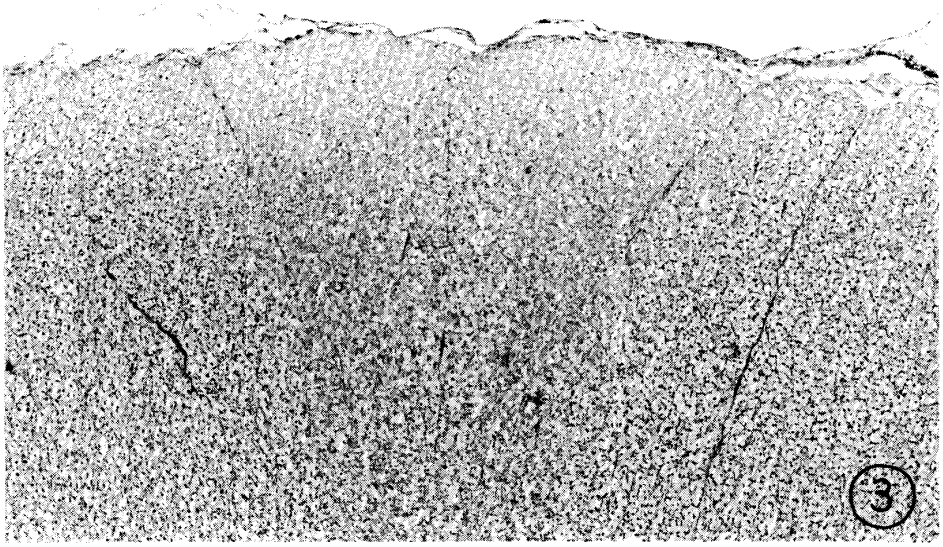

PLATE II

Fig. 4 Intranuclear inclusion showing marginal hyperchromasia in an epithelial cell in a hair bulb.

a) Orderless aggregation of extremely numerous minute particles in the nucleus. x 17,000

b) Higher magnification micrograph showing minute particles of uniform size and an irregular-shaped electron dense amorphous substance resembling a fleecy cloud, of which a number of the particles are clustered together in close contact with each other. x 85,000

c) Connection of intranuclear inclusion and cytoplasm probably at the nucleo-pore. The particles (arrows) are present in this region. x 43,200

Fig. 5 a, b) Intranuclear inclusion bodies (arrow) with loss of karyoplasm a) x 6,600 b) x 7,000

c) The intranuclear inclusion is composed of extremely numerous minute particles and slender filaments of about 2 nm in diameter ; the filaments exhibit irregular distribution and direction patterns. x 80,000

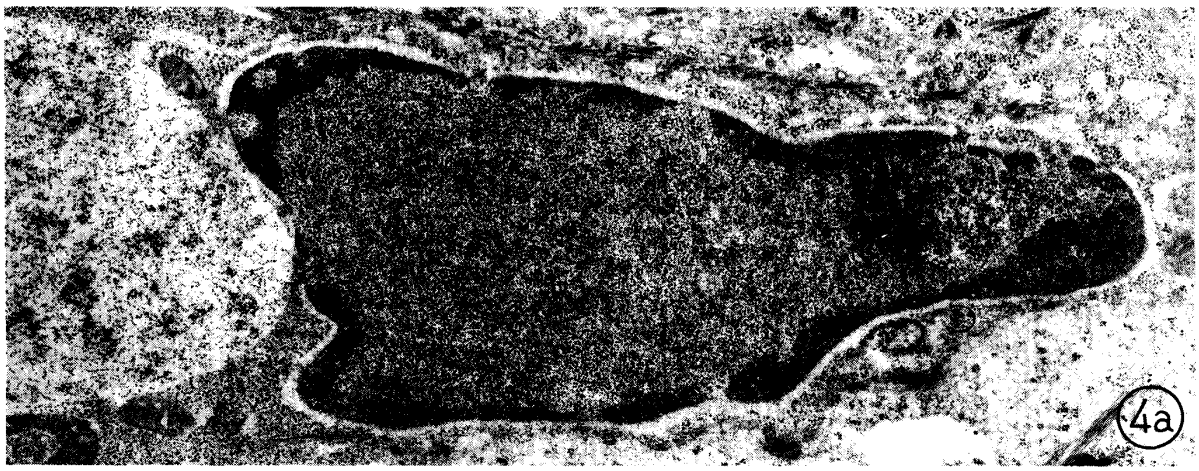
4a

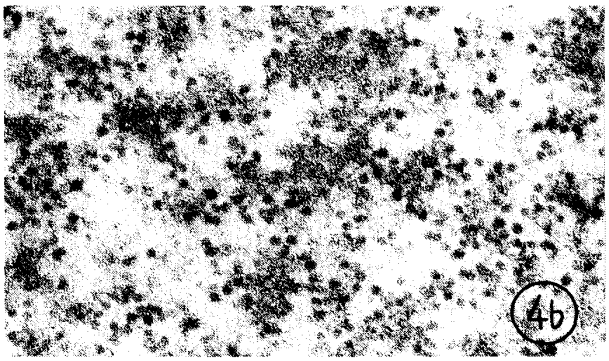
4b

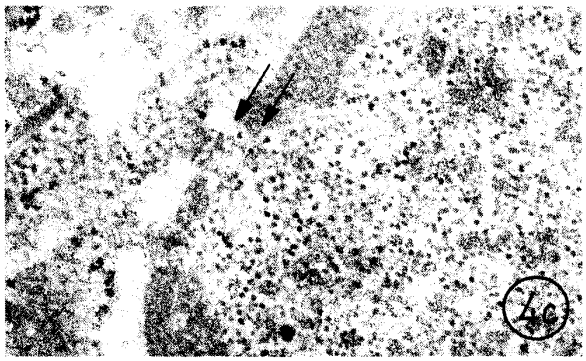
4c


5a

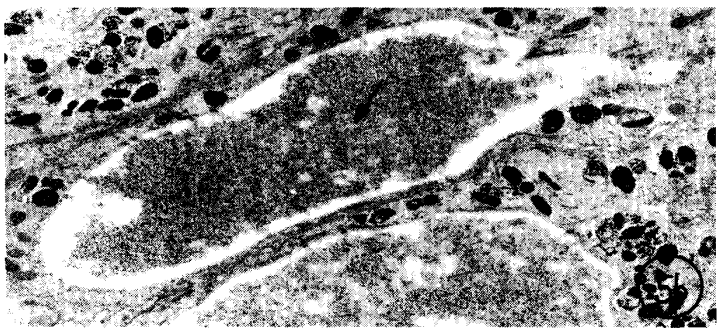
5b

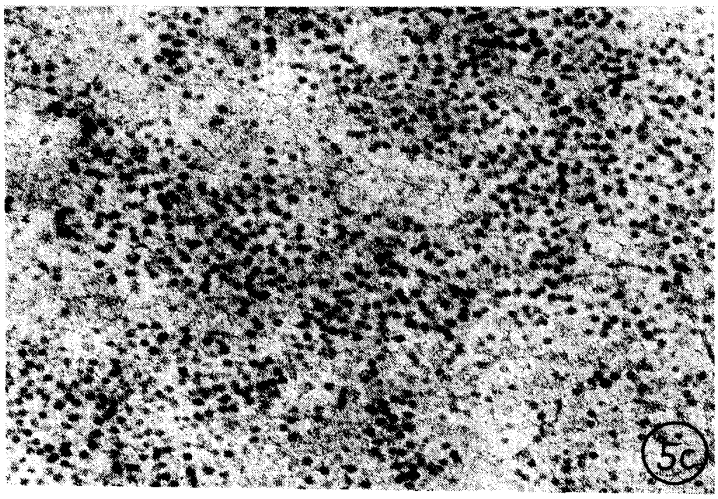
5c

PLATE III

Fig. 6 a) Globular structure in cytoplasmic inclusion. x 22,400
b) Higher magnification micrograph shows the particles aggregated densely in a partially crystalline array. x 84,700
c) Electron dense amorphous substances within globular inclusion. x 79,500

Fig. 7 a, b) Polygonal crystaline structure in cytoplasmic inclusion. Particles arranged regularly in crystalline array and in close proximity to the dense amorphous substance.
a) x 142,000, b) x 154,000

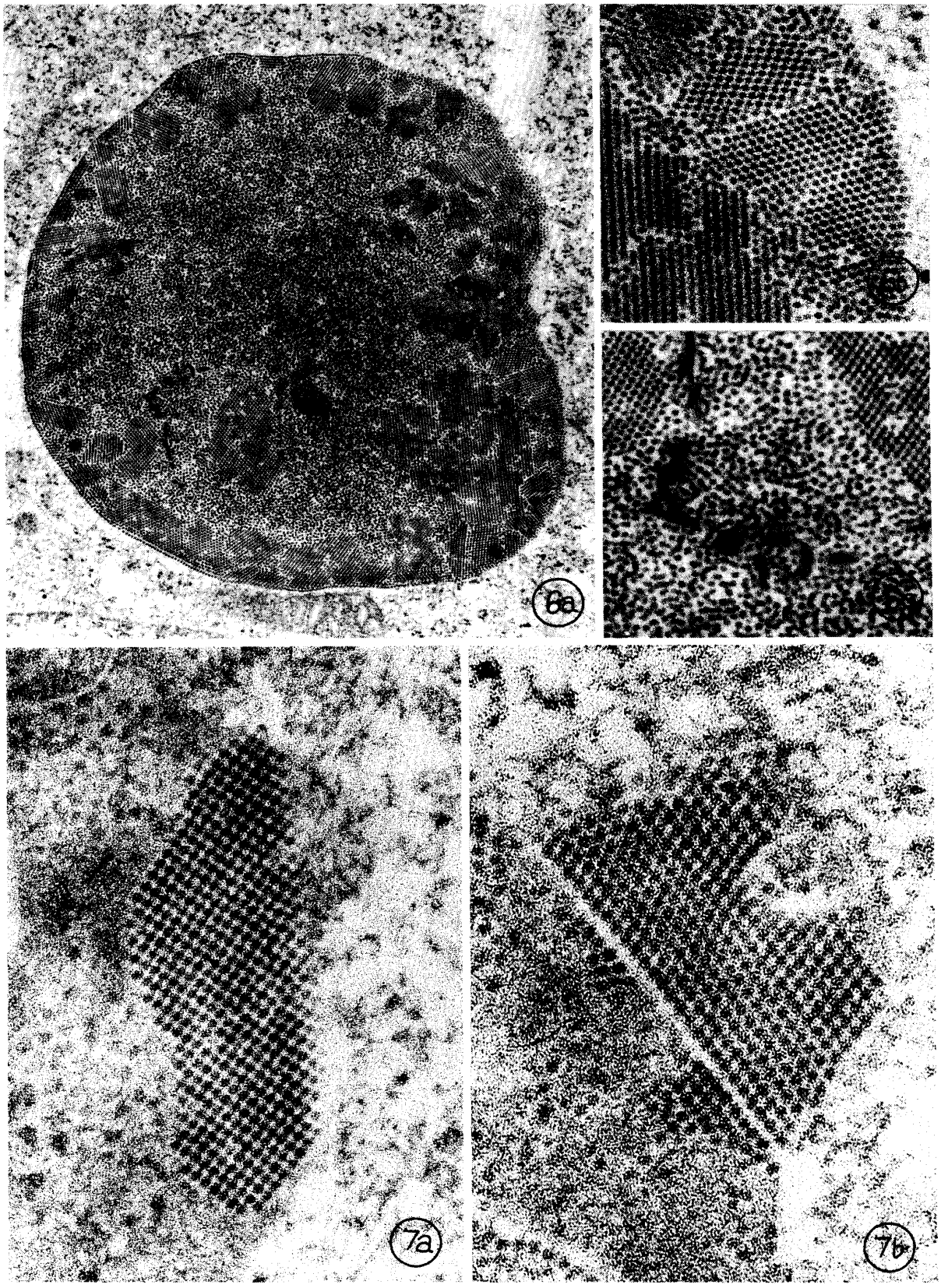
6a
7a
7b

PLATE IV

Fig. 8 Ringed structure in cytoplasmic inclusion.
a) Low power views. N: Nucleus x 36,000
b) Higher magnification micrograph shows a dense amorphous substance resembling a fleecy cloud. The minute particles are arranged in a single line along its border. x 64,000
c) Ringed structures in which the particles are arranged in a single line along a cytoplasmic membrane. x 73,000

Fig. 9 Ovoid structures in cytoplasmic inclusion.
The structure consists of electron dense amorphous substances, along whose border the minute particles are arranged in single or multiple lines. The structure resembling a fleecy cloud (arrow) and containing the particles is also seen. x 85,000

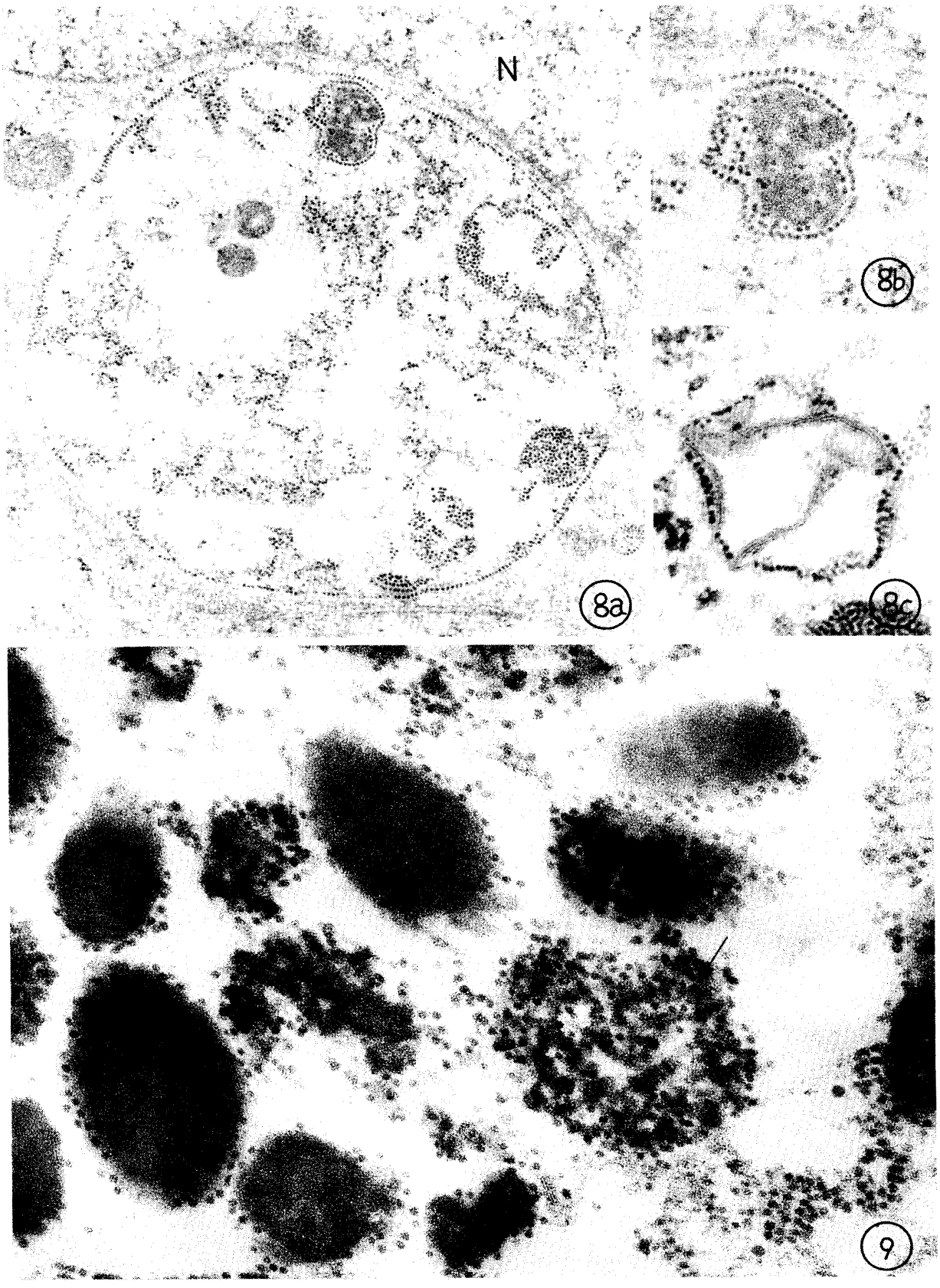
N
8a
8b
8c
9

PLATE V

Fig. 10 a) Higher magnification micrographs show the hexagonal outline of the minute particles (arrow head) ; there is no tail. x 410,000
b) Outline of icosahedral model viewed along the three fold symmetry axis.
c) Outline of icosahedral model viewed along the two fold symmetry axis.
d) Outline of dodecahedral model viewed along the three fold symmetry axis.
e) Outline of dodecahedral model viewed along the two fold symmetry axis.
Hexagonal outline of the particle (arrow head) is similar to (b).

Fig. 11 a) Hexagonal array of minute particles in cytoplasmic inclusion. x 162,000
b) Square array in cytoplasmic inclusion. x 162,000
c) Higher magnification of hexagonal array.
The center-to-center distance between adjacent particles in the hexagonal lattice is almost the same. x 324,000
d) The center-to-center distance between adjacent particles in the square array is almost the same. x 320,000

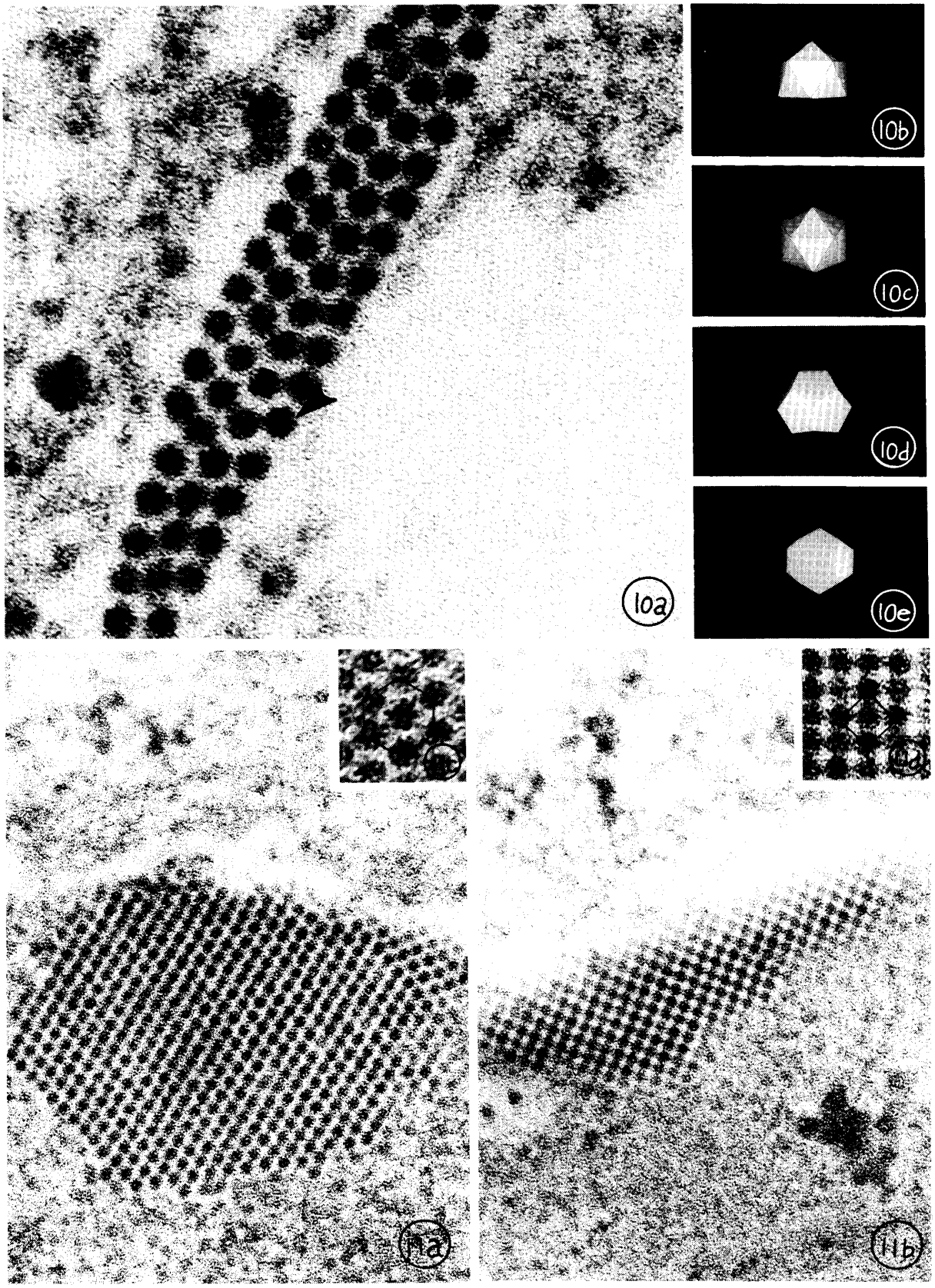
10a
10b
10c
10d
10e
11a
11b

PLATE VI

Fig. 12 Higher resolution micrographs of the minute particles resolve readily the morphological units of 2–3 nm in diameter. Compared with the icosahedral model, in which each of the vertexes was occupied by one black plastic ball, the arrangement of the units (a1) coincides with the icosahedral model (a2) viewed along an inclination of about 10.8 degrees against the five fold symmetry axis. The arrangement (b1 and b2) coincides with the model viewed along the two fold symmetry axis (b3). The arrangement (c1 and c2) coincides with the model viewed along the three fold symmetry axis (c3).
a1) x 925,000, b1) x 1,012,000, b2) x 862,000, c1) x 692,000, c2) x 1,124,000

Fig. 13 a) Extracellular particles (arrows) with no unit membrane in the interepithelial space of the external root sheath. x 69,000
b) Similar particles (arrows) are also seen in the connective tissue around the hair bulb. x 42,000

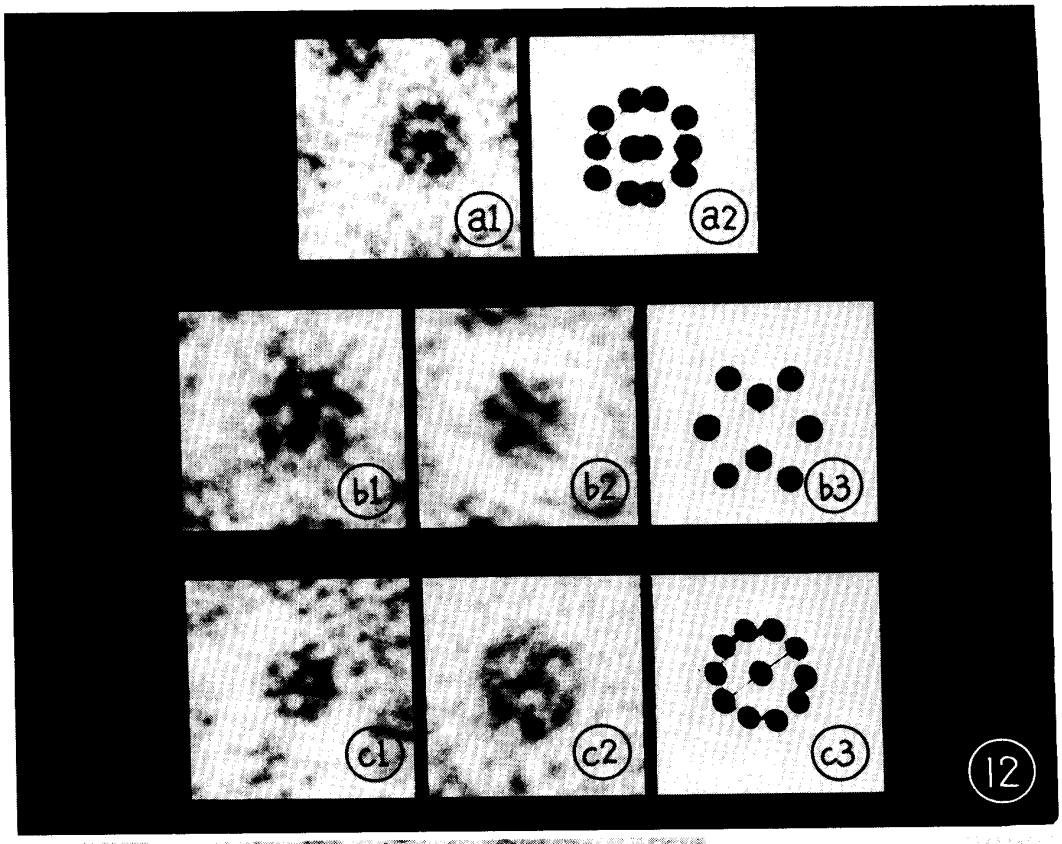
a1
a2
b1
b2
b3
c1
c2
c3
12

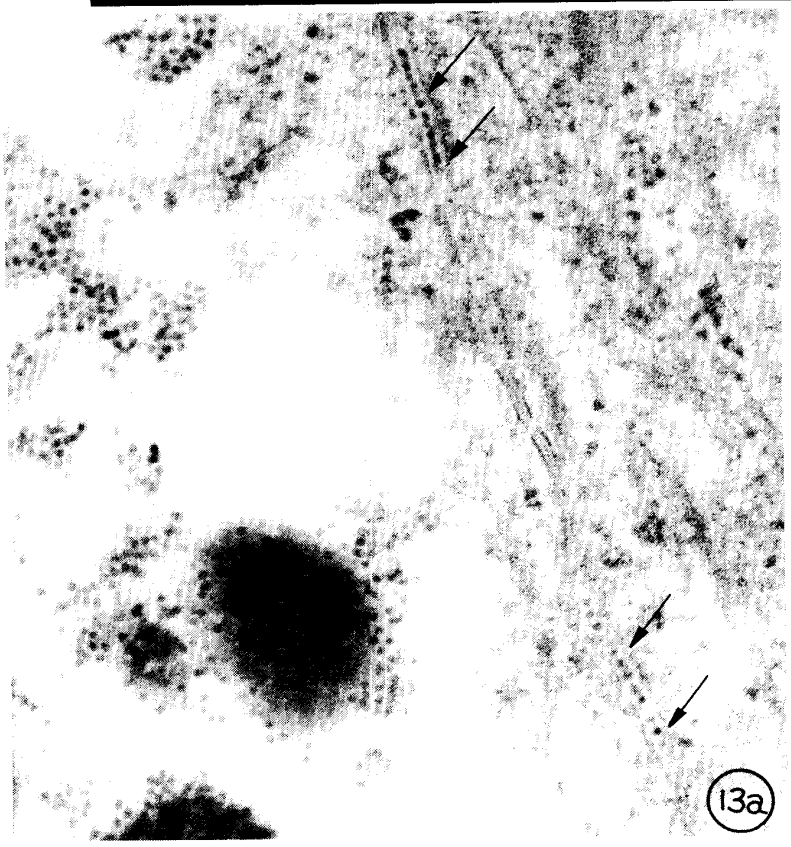
13a

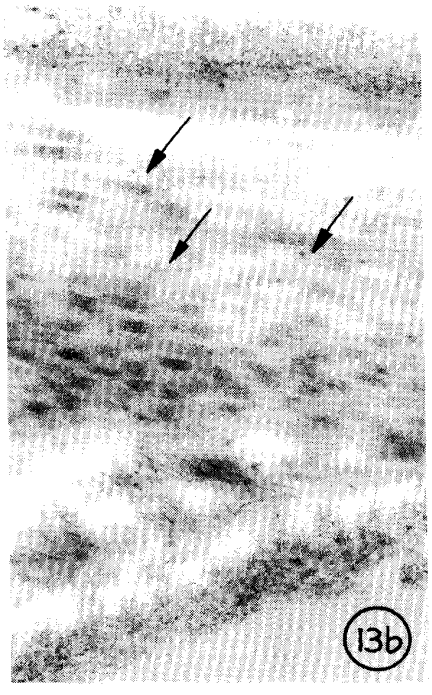
13b